ELSEVIER

Journal of Nuclear Materials 307–311 (2002) 951–955

journal of nuclear materials

www.elsevier.com/locate/jnucmat

Study of point defect behavior in V–Ti alloys using HVEM

T. Hayashi *, K. Fukumoto, H. Matsui

Institute for Material Research, Tohoku University, Katahira 2-1-1, Aoba-ku, Sendai, 980-8577 Japan

Abstract

Microstructural evolution and point defect behavior in vanadium, V–5Ti binary alloy and V–4Cr–4Ti alloy have been examined by using a high voltage electron microscope. In order to examine the effects of interstitial impurity atoms, V–Ti alloys with different levels of purity have also been examined. During irradiation, interstitial-type dislocation loops formed and grew in all of the materials. In alloys, the loop number density (C_L) was much higher than that in vanadium. In high purity V–4Cr–4Ti, contrary to results from our previous study on vanadium, C_L did not significantly decrease or change by purification, indicating solute atoms themselves strongly trap self-interstitial atoms (SIAs). From the temperature dependence of loop density in V–4Cr–4Ti, the effective migration energy of a SIA of 0.50 eVwas obtained. Various observed phenomena are discussed in terms of this activation energy.

1. Introduction

Vanadium-based alloys are considered as one of the candidate structural materials for fusion reactors because of their attractive properties such as low radiation-induced activation, high thermal conductivity, low thermal expansion and superior resistance against radiation-induced swelling [1,2]. In particular, vanadium-based alloys containing titanium as a major alloying element have attractive material properties, represented by high swelling resistance. In these alloys, however, point defect processes relevant to the formation and evolution of secondary defects during irradiation have not yet been fully understood. In order to evaluate material performance after severe, and often non-steady, irradiation conditions, fundamental point defect parameters such as migration energy are essential. Moreover, it is also important to clarify the mechanisms of strong swelling resistance in V–Ti alloys [3].

On the other hand, it is well known that titanium solutes in vanadium strongly scavenge interstitial impurity atoms because of the strong chemical affinity between them [4]. In order to extract the effects of the titanium solute itself and to clarify those of interstitial impurities in V–Ti alloys, highly purified specimens were examined. The main purpose of this study is to obtain further understanding of point defect behavior, some fundamental mechanisms of microstructural evolution and the effects of impurity atoms and titanium solutes.

2. Experimental procedure

Vanadium with 99.9% purity, V–5(at.%)Ti and V–4(at.%)Cr–4(at.%)Ti were prepared. In addition to these materials, NIFS heat-I (H-I) of V–4Cr–4Ti, which had been fabricated and distributed by the National Institute for Fusion Science (NIFS), was used. Ingots of these materials were cold rolled to approximately 0.2 and 0.5 mm thick sheets. TEM disks with a diameter of 3 mm were punched from sheet specimens of 0.2 mm thickness for nominally pure specimens.

For the preparation of high purity (HP) specimens, 0.5 mm thick sheet was sandwiched between zirconium foils 0.015 mm thick, and again cold rolled to approximately 0.25 mm thick sheet in order to bond the zirconium foils to the sheet.

All specimens were recrystallization annealed at 1327 K in a vacuum of 2×10^{-4} Pa for two h. During

* Corresponding author. Tel.: +81-22 215 2069; fax: +81-22 215 2066.

E-mail addresses: thayashi@imr.tohoku.ac.jp, hayashi@fusion.imr.tohoku.ac.jp (T. Hayashi).

0022-3115/02/$ - see front matter
PII: S0022-3115(02)01102-9

Table 1
Amount of major interstitial impurities in V–Ti alloys (appm)

	O	C	N	Amount
V–5Ti	1293	216	76	1584
(VM) V–4Cr–4Ti	1592	50	9	1651
(AS) NIFS H-1V–4Cr–4Ti	576	284	320	1180
(HP) NIFS H-1V–4Cr–4Ti	6	13	22	41

this annealing treatment in the zirconium foil bonded specimens, interstitial impurities in vanadium specimen were gettered by the zirconium. After the recrystallization anneal, the zirconium foils were chemically removed in a HF solution. Finally, both types of disk specimens were thinned by electro-polishing for TEM observation.

Chemical composition of the major interstitial impurities is presented in Table 1 [5]. In the (HP) NIFS H-I, the concentration of impurity atoms, particularly oxygen, was drastically reduced.

Electron irradiation and in situ microstructural observations were conducted in a high voltage electron microscope (HVEM) (JEM ARM-1250) of the High Voltage Electron Microscope Laboratory in Tohoku University at an electron acceleration voltage of 1250 kV. The irradiation temperature and damage rate were varied in the range from room temperature to 623 K and from 4.3×10^{22} to 3.6×10^{23} e m^{-2} s^{-1}, respectively.

3. Results

3.1. Defect formation and evolution in vanadium and V–Ti alloys

At temperatures above about 673 K, severe surface contamination and bend contours in thin foil specimens often occurred due to pick-up of environmental impurities, as reported previously [6,7]. The irradiations were therefore conducted below temperatures where specimen degradation occurs. All results in this study were checked for effects of impurity pick-up and analyzed with great care.

Fig. 1 shows a typical microstructural evolution in (a) vanadium, (b) V–5Ti and (c) (VM) V–4Cr–4Ti. In all materials, interstitial-type dislocation loops formed and grew during irradiation in a similar manner. Loop number density increased just during the initial period of irradiation, and soon saturated. In alloys, loop formation was much enhanced and the growth rates decreased with increasing concentration of solutes. It is understood that the significant enhancement of defect formation in (VM) V–4Cr–4Ti is due to the strong trapping effects on self-interstitial atoms (SIAs) of undersized chromium solutes.

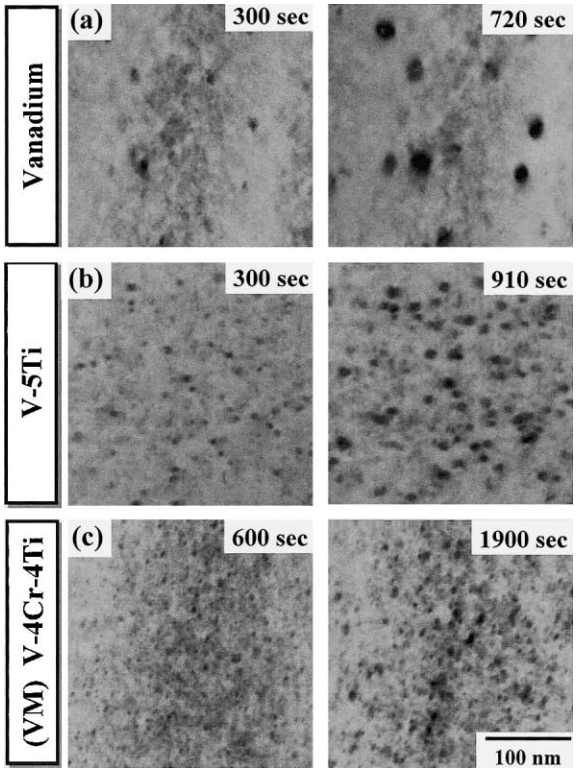

Fig. 1. Typical microstructural evolution in Vanadium (a), V–5Ti (b) and (VM) V–4Cr–4Ti (c) during irradiation at 353 K. Irradiated at an intensity of 1.1×10^{23} e m^{-2} s^{-1} (a) and 2.1×10^{23} e m^{-2} s^{-1} (b) and (c).

3.2. Defect behavior in V–4Cr–4Ti

Examples of defect behavior in (VM) V–4Cr–4Ti, as-received (AS) NIFS H-I and (HP) NIFS H-I are shown in Fig. 2. In all alloys, loops were formed, saturated and grew in a similar manner. Loop density monotonically decreased with increasing irradiation temperature, and the temperature dependence significantly changed at about 453 K.

In the lower temperature region below 453 K, a weaker temperature dependence was observed. Contrary to our initial expectation based on our previous study on vanadium, the loop density in (AS) NIFS H-I with lower concentration of interstitial impurities was higher than that in (VM) V–4Cr–4Ti with higher impurities. Furthermore, the loop density in (HP) NIFS H-I does not substantially decrease or change in comparison with (AS) NIFS H-I. From these results, it appears that interstitial impurities in V–4Cr–4Ti have little effect on loop nucleation.

In the higher temperature region above about 453 K, loop density also shows a temperature dependence, monotonically decreasing with increasing temperature. Its dependence, however, was stronger than that in

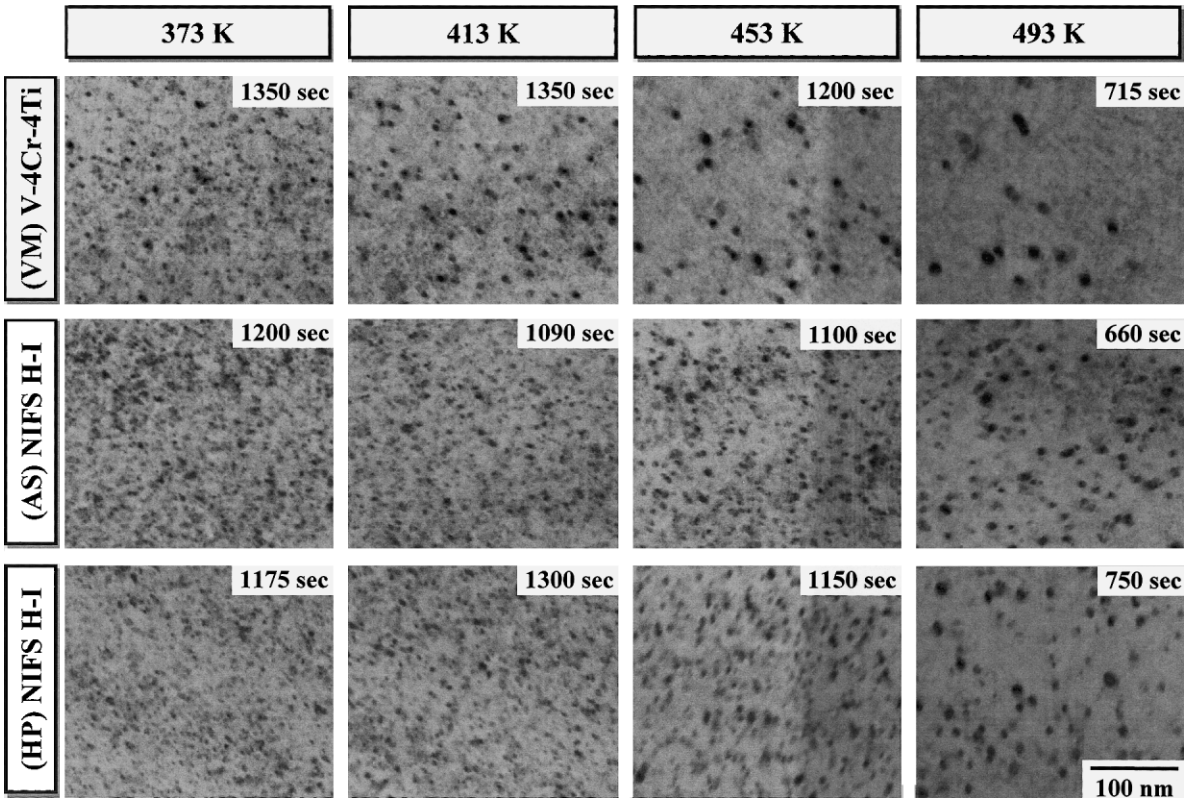

Fig. 2. Damage structures at various temperatures in (VM) V–4Cr–4Ti, (AS) NIFS H-I and (HP) NIFS H-I. Irradiated at an intensity of 2.1×10^{23} e m^{-2} s^{-1}.

lower temperature region. In NIFS H-I, a heterogeneous distribution of defects was observed in this temperature region. Fig. 3 shows an example of the depth distribution of defects in NIFS H-I, examined by taking a pair of stereo micrographs. As seen in the figure, defects were formed preferentially near both surfaces of the wedge-shaped specimen. This heterogeneity became more significant with increasing irradiation temperature.

3.3. Dependence of loop density on irradiation temperature and intensity

Fig. 4 shows an Arrhenius-type plot of the measured loop number density. In V–4Cr–4Ti alloys, the temperature dependence can be divided into two stages; a stage showing weak linear dependence on the inverse of irradiation temperature ($1/T$) below about 453 K, labeled stage III′, and another stage showing strong dependence above 453 K, labeled stage IV. It is likely that the nucleation process in the above two stages, separated at 453 K, differs from one another.

In order to clarify the mechanisms of loop nucleation, irradiation intensity (damage rate) dependence of loop density was examined. Fig. 5 shows the intensity

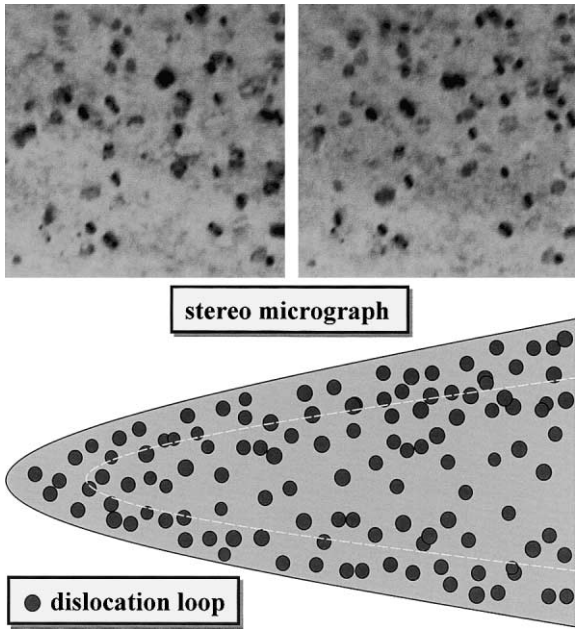

Fig. 3. Schematic presentation of defects distribution in NIFS H-I observed in the higher temperature region (stage IV).

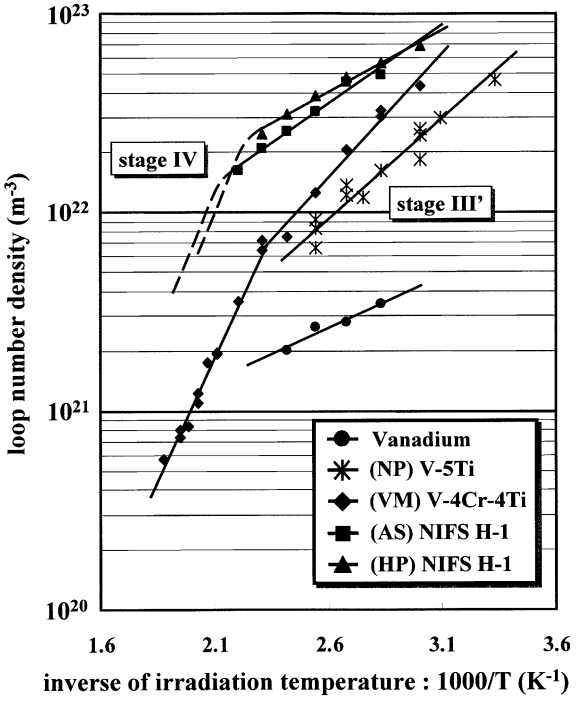

Fig. 4. Arrhenius type plot of loop number density in vanadium and V–Ti alloys.

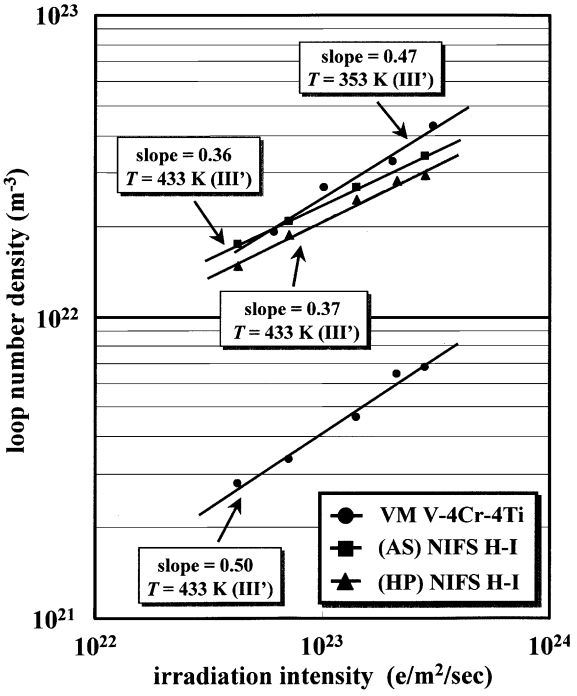

Fig. 5. Irradiation intensity dependence of loop number density in stage III′ (below 453 K) in V–4Cr–4Ti.

dependence at temperatures corresponding to stage III′. In (VM) V–4Cr–4Ti, in both stages, loop density was almost proportional to the square root of the dmage rate. A weaker dependence, however, was observed in both types of NIFS H-I.

4. Discussion

4.1. Interstitial mobility and loop nucleation in V–5Ti and (VM) V–4Cr–4Ti

In order to analyze the data obtained from the HVEM experiments, rate theory equations for loop nucleation have been used, assuming that di-interstitials are stable loop nuclei, as proposed by Yoshida et al. [8]. According to their study, several stages appear in the temperature dependence of loop density when there are strong immobile trapping centers for SIAs in the matrix, and the interaction between them dominates loop nucleation.At higher temperatures where the rate of trapping and detrapping of SIAs by trapping sites become comparable to that of other processes, a saturated loop number density (C_{L}^{∞}) can be described as follows:

$$C_{\mathrm{L}}^{\infty} \propto \left(\frac{PC_{\mathrm{M}}}{M_{\mathrm{B}}}\right)^{1/2} = (PC_{\mathrm{M}})^{1/2} v \exp\left(\frac{E_{\mathrm{M}}^{\mathrm{I}} + E_{\mathrm{B}}^{\mathrm{I}}}{2kT}\right),$$

where P is the production rate of point defects, C_{M} the concentration of impurity atoms, M_{B} the rate of the binding and dissociating reaction between SIAs and trapping sites, $E_{\mathrm{M}}^{\mathrm{I}}$ the migration energy for SIA and $E_{\mathrm{B}}^{\mathrm{I}}$ the binding energy between a SIA and a trapping site.

In (VM) V–4Cr–4Ti, the results in Fig. 5 are in good agreement with this square root dependence on irradiation intensity. This suggests that in stage III′, di-interstitials are effective loop nuclei, and the loop nucleation process in both alloys follows the rate theory predictions.

In V-5Ti and (VM) V–4Cr–4Ti, the trapping sites dominating the loop nucleation in stage III′ are considered to be oversized titanium solutes. Titanium solute is a major alloying element in both alloys, and its relative concentration to those of other solutes is high enough to mask other nucleation processes. Indeed, it is reasonable to consider that strong enhancement of loop density in V–5Ti is due to the trapping effects of titanium solutes on SIAs. Furthermore, the independence of loop density on interstitial impurity concentration, observed in NIFS H-I, seems to support this.

From the slope of the line in stage III′ and stage IV, an activation energy for loop nucleation has been obtained for (VM) V–4Cr–4Ti in each stage of 0.50 and 1.0 eV, respectively. The obtained energy in stage III′ is considered to represent the effective migration energy of a SIA, that is, the sum of the SIA migration energy and

the binding energy between a SIA and a trapping site, i.e. titanium solute.

In stage IV, however, it is difficult to explain the mechanism of the strong temperature dependence in terms of the above introduced rate theory. There are some possible mechanisms, e.g. thermal migration of vacancies and/or thermal decomposition of di-interstitials in this higher temperature region. The investigations to clarify the nucleation process in stage IV and 'pure' titanium effects on point defect behavior are now under way.

4.2. loop nucleation process in NIFS H-I

Formation of a higher density of loops in (AS) NIFS H-I with lower concentration of impurities than that in (VM) V–4Cr–4Ti with higher impurities means that more and/or stronger trapping sites, which are not interstitial impurities and rarely included in (VM) V–4Cr–4Ti, exist in NIFS H-I. Moreover, the result of (HP) NIFS H-I indicates that interstitial impurities rarely have effects on loop nucleation in the lower temperature range in V–4Cr–4Ti.

According to Muroga et. al. [5], several kinds of metallic impurities, e.g. silicon and aluminum, are in higher concentrations in NIFS H-I than in (VM) V–4Cr–4Ti. These impurities have been included through the production process of the large heat. These metal impurities can have strong trapping effects on SIA migration in the temperature region examined in this study, resulting in the strong enhancement of loop nucleation in NIFS H-I. Unfortunately, it is difficult to identify what kinds of impurities act as a trapping sites in NIFS H-I from the results obtained in this study. More detailed investigations on the effects of minor elements, such as silicon and aluminum, and the heterogeneous loop formation in the higher temperature region, are needed to clarify point defect behavior in NIFS H-I.

5. Summary

The microstructural evolution and point defect behavior during irradiation in V–Ti alloys have been studied by using HVEM. Several types of V–4Cr–4Ti specimens with different purity have been investigated.

1. The formation and evolution of SIA-type loops was observed in all materials. In V–Ti alloys, the loop number density was much higher and the loop growth rate was much lower than those in vanadium, indicating strong trapping effects of the solutes on SIAs.
2. Loop density in V–5Ti and (VM) V–4Cr–4Ti was proportional to the square root of irradiation intensity. From this result, it was concluded that di-interstitials are effective loop nuclei in both alloys.
3. The temperature dependence of loop density in V–4Cr–4Ti consists of two stages; a lower temperature region (stage III′) with weak temperature dependence and higher temperature region (stage IV) with strong dependence. From the temperature dependence in stage III′, the effective migration energy of a SIA was determined to be 0.50 eV, for (VM) V–4Cr–4Ti.
4. Loop density in NIFS H-I with lower concentration of interstitial impurity was higher than that in (VM) V–4Cr–4Ti with higher concentration of impurities. It is considered that metal impurities in NIFS H-I act as strong trapping sites of SIAs, enhancing loop nucleation.
5. Loop density in (HP) NIFS H-I did not significantly decrease or change. This is an evidence that at least in the stage III′, interstitial impurities in V–4Cr–4Ti have little effect on loop nucleation.

Acknowledgements

The authors are deeply indebted to E. Aoyagi and Y. Hayasaka in High Voltage Electron Microscope Laboratory in Tohoku University for their technical assistance in using HVEM. The help in the high purity specimen preparation by Mr K. Takahashi is also greatly appreciated. The authors also would like to thank Professor T. Muroga and Dr T. Nagasaka for supplying the NIFS H-I specimens. Also we would like to thank research foundation for the electrotechnology of Chubu for the financial help.

References

[1] H. Matsui, K. Fukumoto, D.L. Smith, H.M. Chung, W. VanWitzenburg, S.N. Votinov, J. Nucl. Mater. 233–237 (1996) 92.
[2] H.M. Chung, B.A. Loomis, D.L. Smith, J. Nucl. Mater. 239 (1996) 139.
[3] B.A. Loomis, D.L. Smith, J. Nucl. Mater. 191–194 (1992) 84.
[4] T. Shikama, S. Ishino, Y. Mishima, J. Nucl. Mater. 68 (1977) 315.
[5] T. Muroga, T. Nagasaka, A. Iiyoshi, A. Kawabata, S. Sakurai, M. Sakata, J. Nucl. Mater. 283–287 (2000) 711.
[6] T. Hayashi, K. Fukumoto, H. Matsui, J. Nucl. Mater. 283–287 (2000) 234.
[7] T. Muroga, K. Araki, N. Yoshida, ASTM-STP 1047 (1990) 199.
[8] N. Yoshida, M. Kiritani, F.E. Fujita, J. Phys. Soc. Jpn. 39 (1975) 170.